Research Article GU J Sci 34(2): 406-421 (2021) DOI: 10.35378/gujs.752304

Gazi University

Journal of Science

http://dergipark.gov.tr/gujs

Greener Approach to Synthesis of Steady Nano-sized Gold with the Aqueous Concentrate of *Cotinus Coggygria Scop*. Leaves

Mahmure USTUN OZGUR*, Ebru ORTADOGULU, Burak ERDEMIR

Yildiz Technical University, Faculty of Science and Art, Department of Chemistry,34220 Istanbul, Turkey

Highlights

- The current study reports an economical and simple technique for biosynthesis of gold nanoparticles.
- Developed procedure avoids utilization of harmful and poisonous solvents.
- Cotinus Coggygria Scop.leaves (CCSL) extract behaved as a bio-decreasing and stabilizing factor.
- Obtained gold nanoparticles (CCS-AuNPs) are stable, fluorescent, sphere-shaped and in size ~17 nm.

Article Info

Received:13 June 2020
Accepted:09 Nov 2020

Keywords

Green synthesis
Gold nanoparticles
Cotinus coggygria
Fluorescent
Antibacterial activity

Abstract

There is a growing commercial attraction for nanoparticles because of their widespread feasibility in various fields for instance electronics, textiles, chemistry, medicine, energy and catalysis. This investigation describes an environmentally benign, cheap, and simple technique for biosynthesis of CCS-AuNPs utilizing the CCSL aqueous concentrate as a covering and reducing material. Various parameters influencing the reduction of Au^{3+} to Au^{0} were studied and the optimum conditions found as follows: chloroauric acid solution: 1 mM, CCSL aqueous extract: 20 g dry leaf /250 mL distilled water, volume proportion of chloroauric acid solution to CCSL aqueous solution: 24.8/0.2, pH: 3, response temperature: 60°C, and response time: 15 min. By stirring the reaction combination at 60°C for 10-15 minutes, the CCSL aqueous extract reduced Au^{3+} ions to Au^{0} and production of CCS-AuNPs was observed with the change of CCSL extract colour from light yellow to dark purple. Produced CCS-AuNPs were well defined by Ultraviolet-visible (UV-vis) absorption spectroscopy, Fourier Transform Infrared Spectroscopy (FTIR spectroscopy), and Transmission electron microscopy (TEM). In the absorption spectrum, a symmetrical and prominent band observed in 500-600 nm wavelength range indicated that CCS-AuNPs formed. Synthesized gold nanoparticles at the optimum conditions are spherical (average particle size~17 nm) and remained stable for four months. Gold nanoparticles showed two fluorescent emission peaks at 444 nm and 704 nm whenever induced at 350 nm. Synthesized CCS-AuNPs showed lower antibacterial effect than plant extract.

1. INTRODUCTION

Recently, interest in metal nanoparticles has increased because of their different chemical, biological and physical features, and has become the most effective research and development area [1]. Production (bio-synthesis, green procedure) of various metal and metal oxide nanoparticles by utilizing concentrate of different parts of plants ensures advancement and improvement compared to other methods with their features such as easy, one step, low cost, environmentally friendly and relatively reproducible [2]. Nanoparticles have applications in numerous fields, for example, the food industry, medication distribution, biomedical, health, environment, optics, space industry and tissue engineering [3].

Nanoparticle synthesis could be achieved through numerous physical and chemical techniques, however, usage of these kinds of techniques are hazardous in somehow. Green synthesis has attracted more relevance owing to the increasing necessity to improve ecologically benign techniques in material production [4]. This encouraged searchers to produce the metal and metal oxide nanoparticles with green procedures that permit better check of particle dimension and shape for different implementations. The extract of various

*Corresponding author, e-mail: mozgur@yildiz.edu.tr

parts of plants could behave as a reducing, covering and stabilizing component in the synthesis of varied nanoparticles. An effective antibacterial efficiency of gold nanoparticles (AuNPs) and rapid reduction of the Au-salt solutions have benefited the green production of AuNPs more popular using the extracts of different parts of plants. AuNPs appear as encouraging compounds for cancer remedy, and nano-dimensional AuNPs have been assessed for different kinds of humans cancer cells. Often, phytochemical compounds in different parts of plants (roots, leaves, flowers and fruits) such as phenols, flavonoids, amino acids, aldehydes, alkaloids, ketones, terpenoids can take part in the bio-reduction of $[AuCl_4]^-$ ions [5]. Previously, it was reported that plant concentrates containing these phytochemicals have been used for the green synthesis of metal nanoparticles [6-8]. Various plants used for the production of AuNPs by green procedure in recent years are given in Table 1. In order to make possible the nanoparticle synthesis with the green methods to contest with the chemical techniques, quicker synthesis is needed. This study was conducted on a more environmentally friendly and fast production of AuNPs. The exact reduction of $[AuCl_4]^-$ ions occurred in around 15 minutes. As seen in Table 1, the time required for green synthesis is shorter than the other studies. In addition, when compared with other studies in Table 1, very small (~17nm) particle-sized gold nanoparticles were obtained in our study and these small nanoparticles remained stable for four months without aggregates.

Table 1. *Some recent studies for the green production of AuNP using plants*

Sample no	Extract of plant	Particle size (nm)	Particle shape	Synthesis time	References
1	*Onion (Allium cepa)*	~100	spherical and cubic	1h	[9]
2	*Sumac*	15-25	spherical	at 40 ˚C 40 min and 1 h at ambient temp.	[10]
3	*Amaranthus spinosus*	~ 11	spherical and triangular	not stated	[11]
4	*Prunus domestica gum*	7-30	mostly spherical	at 40 ˚C 80 min	[12]
5	*Black Cardamom*	25-35	different shapes and sizes	10-20 min	[13]
6	*Elettaria cardamomum*	15-25	spherical	5 min	[14]
7	*Galaxaura elongata*	3.85-77.13	spherical	3 h	[15]
8	*Magnolia and Diopyros kaki*	5-300	plate and spherical	at 95 ˚C few min	[16]
9	*Mango peel*	6-18	quasi- spherical	40 min	[17]
10	*Olive leaf*	50-100	triangular and spherical		[18]
11	*Pistacia integerrima gall*	20-200	not stated	not stated	[19]
12	*Salix alba*	50-80	not stated	not stated	[20]
13	*Nerium oleander*	2-10	spherical	at room temp 20 min	[21]
14	*Cotinus coggygria*	~17	spherical	at 60°C for 10-15 min	current study

Cotinus Coggygria Scop. (CCS) has a place in the *Anacardiaceae* family and is often referred to as a smoke tree. It is a trading decorative tree with extreme therapeutic uses [22]. Various pieces of the CCS tree have been exposed to pharmacological assessment for the anti-inflammatory, hepatoprotective, antiseptic and antimicrobial effects [23]. The concentrate of the CCS bark is utilized to cure cancer cells in Serbian folk medicine [24]. In different nations, CCS leaves are used in manufacturing an essential oil for use in perfumery [25]. The main phytochemical active ingredients in ethyl acetate and methanol concentrates of different pieces of the CCS plant have been found to be phenols, tannins and flavonoids. Šavikin et al. reported that the main components in the HPLC analysis of the CCS flower and leaf extracts were gallic acid and its derivatives [26].

Utilization of CCS leaves aqueous extract for green production of CCS-AuNPs has not been declared yet.

In this research, green production of CCS-AuNPs was successfully performed utilizing the aqueous concentrate of CCS leaves. We researched the effects of the reaction circumstances such as the volume ratio of auric acid solution to CCSLE, reaction temperature, synthesis time and pH on the steady and particle size of synthesized CCS-AuNPs. The produced CCS-AuNPs were defined using UV–vis spectroscopy, transmission electron microscopy and Fourier transform infrared spectroscopy techniques. Antibacterial and fluorescence properties of produced CCS-AuNPs were also investigated.

2. MATERIAL METHOD

2.1. Reagents and Apparatus

Chloroauric acid ($HAuCl_4.3H_2O$, 99.9%) was purchased from Sigma-Aldrich. 0.17g of $HAuCl_4.3H_2O$ dissolved in 500 mL distilled water to prepare the stock solution. In this study, ethanol, gallic acid, α-tocopherol, trichloroacetic acid (TCA, 10%, w/v), sodium carbonate (2%, w/v), folin-ciocalteu reagent (F-C), ferric chloride ($FeCl_3$, 1%, w/v), 1,1-Diphenyl-2-picryl hydrazyl (DPPH), butylated hydroxyanisole (BHA), butylated hydroxytoluene (BHT), phosphate buffer (pH6.6), and potassium ferricyanide [$K_3Fe(CN)_6$] were of analytical purity. CCS leaves (Figure 1) were collected from Edirne in July from their natural bindings and washed with deionized water to eliminate the impurities. The cleaned CCS leaves were desiccated in shadow at 20-25°C and stored in a dry place for use in the experiments.

Figure 1. *Digital photographs of C. Coggygria Scop. that used in this study*

All spectral measurements and treatment of data were accomplished on a twofold bar Shimadzu UV- 1800 spectrophotometer (Japan) and UV-probe 2.35 software was used to process the absorption spectra. All spectra were recorded over the range of 350-720 nm. Fluorescence measurements were performed using a Varian Eclipse spectrofluorometer. TEM studies were implemented on a JEOL JEM 2100 HRTEM working at 200 kV. Pictures were taken by Gatan Model 794 slow-scan CCD camera and furthermore by Gatan Model 833 Orius SC200D CCD camera. Carbon bolster film covered copper TEM grids (Electron Microscopy Sciences, CF200-Cu, 200 mesh) were utilized. FTIR spectra of CCSL extract and CCS-AuNPs were documented with a Perkin Elmer FTIR (ATR sampling accessory) spectrophotometer. The bacterial cultures selected for the present study were *E. coli* (ATCC 25922) and *S. aureus* (ATCC 25923).
All microorganisms were preserved on specific media slants at 4°C and revitalized before use. Logarithmic phase bacterial inoculums (10^8 cfu/mL) were standardized against McFarland standard.

2.2. Preparation of *C. Coggygria Scop* Leaves Extract

Leaves were chopped into small pieces. About 25 g of chopped CCS leaves was transferred into 400 mL erlenmeyer having 250 mL deionized water. It was thoroughly mixed and boiled at 80°C for 60 min. Filtered concentrate was left to cool and centrifuged at 5000 rpm for 15 min at 20-25°C, then filtered to eliminate each suspended granules. A clear concentrate was achieved, and its volume was diluted to 250 mL. Obtained CCSL aqueous concentrate was kept in a dark place at 4°C for one month for use in subsequent experiments.

For the extraction with ethanol, 20 g of chopped plant material was stirred with 350-400 mL ethanol and extracted for 3 hours using a magnetic stirrer under room conditions. The obtained extract was filtered through a filter paper (Whatman No.2) and vaporized by using a vacuum rotary evaporator at 40ºC.

2.3. Determination of Phenolic Compound Concentration in CCSL Ethanol Concentrate

The phenolic compound concentration of the ethanol concentration of the CCSL was assayed by Folin-Ciocalteu procedure and calculated as milligram gallic acid per gram of concentrate [27]. 1 mL of CCSLE extract and 40 mL of deionized water were transferred to a 50 mL measuring flask, after that 1 mL of pure F-C reagent was also transferred to the solution. After 3 minutes, 2 mL Na_2CO_3 solution was transferred and completed to volume with deionized water. After 2h incubation in a shaker water bath at 25ºC, the absorbance values of the samples were measured versus blank (solution having deionized water instead of sample) at 760 nm wavelength. Gallic acid calibration curve (prepared at various concentrations: 50-250 µg/mL) was used to determine phenolic contents. The obtained results were calculated as the averages of three separate studies.

2.4. Assay of Antioxidant Efficacy of CCSL Ethanol Concentrate

The antioxidant efficacy of CCSL concentrate was determined using DPPH radical scavenging procedure [28]. 4 mL of 0.1 mM DPPH reagent (prepared in ethanol) was transferred to 1 mL of plant extracts of different concentration (concentration range: 10 µg/mL - 500 µg/mL), separately. Prepared solutions were incubated in the dark place for 30 min at 25°C and the absorbance values were evaluated at 517 nm. The percentage of DPPH decolourisation of the solutions was computed in accordance with Equality (1)

$$\text{DPPH decolourisation \%} = 1-(Ass/Acs)]\times 100 \quad (1)$$

where Ass is the absorbance value of sample solution and Acs is the absorbance value of control solution.

The procedure developed by Dehpour et al. [29] was applied to assay the reduction capability of the ethanolic extract of CCSL. 1mL of clear concentrate at different concentrations (concentration range from 50 µg/mL to 250 µg/mL) was transferred to the mixture containing 2.5 mL of potassium ferricyanide and 2.5 mL of phosphate buffer. Prepared solutions were incubated for 20 minutes at 50°C and 2.5 mL of TCA solution was transferred to the mixture. Obtained mixtures were centrifuged for 10 minutes at 3000 rpm. 2.5 mL of supernatant solution was transferred to the mixture containing 2.5 mL deionised water and 0.5 mL $FeCl_3$ reagent. Absorbance values were evaluated at 700 nm wavelength against the blank (having deionised water instead of sample) solution. Increased absorbance values of the sample solutions demonstrate the increased reducing capability. Three reproduces were accomplished for each sample and mean value was calculated.

2.5. Synthesis of Gold Nanoparticles

Various volumes (0.1, 0.2, and 0.5 mL) of the aqueous extract of CCSL were combined with chloroauric acid solution and total volume was completed to 25 mL with $HAuCl_4$ solution. The prepared solutions were kept on a magnetic stirrer with 250 rpm at 25°C. Depending on the volume of the CCSL extract, the color of the colloidal solution returned from light yellow to purple and dark purple with the reduction of Au^{3+} to Au^0. The absorption spectra of the solutions were measured against distilled water. Diagrammatic representation of gold nanoparticle synthesis was given in Figure 2.

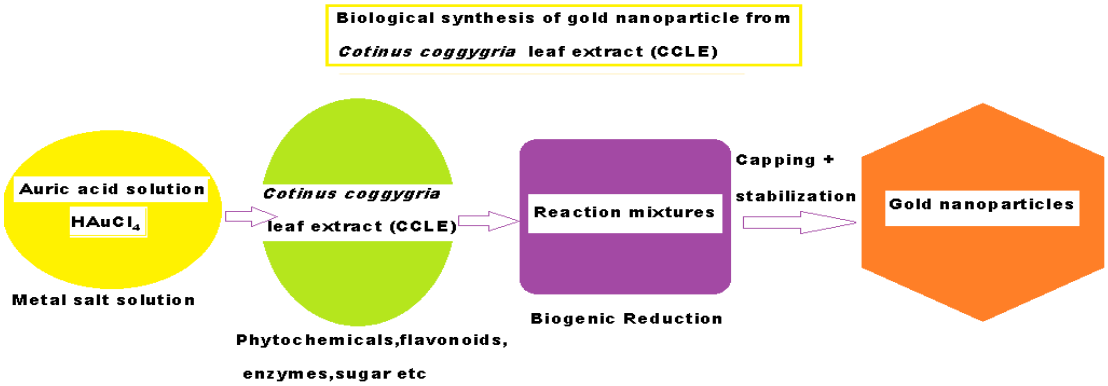

***Figure 2**. Diagrammatic representation of gold nanoparticle synthesis*

2.6. Effect of Various Parameters on the Production of CCS-AuNPs

In this study, different parameters identified as factors affecting the synthesis yields of Au-NPs, including reaction temperature, pH, reaction time and volume ratio of $HAuCl_4$ solution to CCSL extract were studied and optimized.

To optimize the volume ratio of chloroauric acid solution to CCSL extract for the maximum production of stable CCS-AuNPs, the synthesis procedure (Section 2.5) was repeated with different volume ratios (24.5: 0.5, 24.8: 0.2 and 24.9: 0.1 v/v).

To investigate the reaction time required for the finalization of reaction, 0.1, 0.2 and 0.5 mL CCSL extract was decanted into a 25 mL volumetric flask and completed to the volume with 1 mM $HAuCl_4$ solution. The synthesis procedure (Section 2.5) was followed and the formation of nanoparticles monitored by taking the absorption spectra of samples taken from the solution at certain intervals for 5 h.

To optimize the reaction pH on the production of the CCS-AuNPs, a series experiment set was separately carried out with the chloroauric acid solution which having different pH values (from pH3 to pH 11). pH of the 1 mM $HAuCl_4$ solution was set to pH3 by adding drop by drop of 0.1N NaOH or 0.1N HCl solutions. 0.2 mL CCSL extract was transferred to 25 mL volumetric flask, made up to the volume with 1 mM $HAuCl_4$ (pH3) solution and stirred at 250 rpm and 25°C. To optimize the reaction pH, the above- mentioned method was repeated for solutions where the pH of 1 mM $HAuCl_4$ solution was adjusted to 5, 7, 9 and 11. After 3 h, absorption spectra of the samples were taken and absorbance values were measured at maximum wavelength.

To research, the impact of the reaction temperature on the production of the CCS-AuNPs, the synthesis procedure (Section 2.5) was repeated at 30, 60 and 90°C temperatures. At the applied temperatures, the reactions were carried out at 250 rpm and color change was observed as a consequence of the reaction formed. Reducing of Au^{3+}ions to Au^0 was observed by measuring the absorption spectra of the samples taken from the reaction medium at 15-minute intervals for 1 hour.

2.7. Antibacterial Efficacy of Biosynthesized CCS-AuNPs and CCSL Extract

The agar well diffusion technique was utilized to inspect the antibacterial efficacy of biosynthesized CCS-AuNPs and CCSL extract on chosen reference bacteria (gram-negative *E. coli* and gram-positive *S. aureus*)[30]. For this purpose, logarithmic phase bacterial inoculums (with a density of 108cfu/mL) were standardized against the MacFarland standard. Utilizing a sterile cotton swab, the nutritive agar plates were swabbed uniformly with reference bacteria from fresh cultures. With the assistance of sterile gel perforation, wells of around 6mm diameter were performed onto the agar sheets. 30 µL of CCS-AuNPs solution or CCS leaf extract was transferred to the wells drilled using a sterile micropipette. In the

experiments, a well filled with sterile distilled water was used for control. After the culture plates were incubated for 24 hours at 37 °C the inhibition zone diameters were evaluated.

3. THE RESEARCH FINDINGS AND DISCUSSION

3.1. Determination of Phenolic Content and Antioxidant Activity CCS Leaves

The phenolic content of the ethanolic extract of CCSL, calculated as gallic acid equivalents (GAE), was 168 ± 0.04 mg GAE /g CCSL.

By utilizing a stable DPPH free-radical, the ethanol extract of CCSL was analyzed for free-radical scavenging ability. With the purpose of compare the DPPH scavenger ability of the ethanol extract of CCSL, synthetic antioxidants such as BHA and BHT were employed. DPPH radical cleaning abilities of the ethanol extract of CCSL, BHA and BHT standards are shown in Figure 3. Lower absorbance values demonstrate the higher radical scavenging abilities. The obtained values were calculated by taking the average of three separate studies. The maximum inhibition percentage value of the ethanol extract of CCSL is 91.71±3.40% at the concentration of 50µg/mL. The percentage inhibition values of the BHA used as standard were equal to those of the ethanol extract of CCSL and the percent inhibition values of BHT were lower than those of the CCSL ethanol extract.

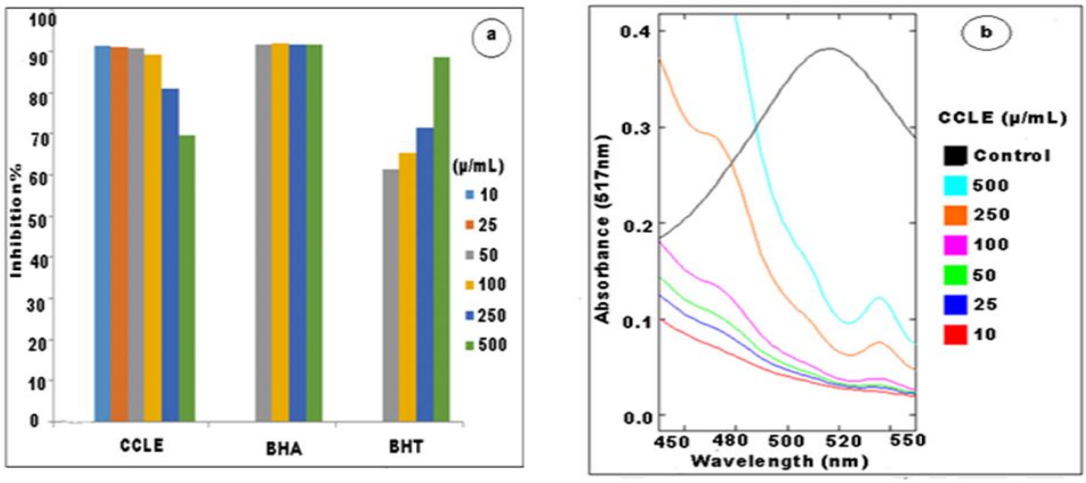

Figure 3. (a) *The comparative free radical scavenging abilities of CCSL ethanol concentrate, BHA and BHT,* ***(b)*** *absorption curves obtained from DPPH radical scavenging capability experiments*

α-tocopherol and BHT were utilized as positive control for determining the reducing power of the ethanol concentrate of CCSL. While the maximum absorbance value for the ethanol concentrate of CCSL was 1.92 for 250µg/mL, it was measured as 1.01 and 0.99 for the same concentration of α-tocopherol and BHT standards, respectively (Figure 4). The sequence of reduction abilities of ethanol extract of the CCSL and standard solutions is as follows; CCSL ethanol extract> BHT = α-tocopherol.

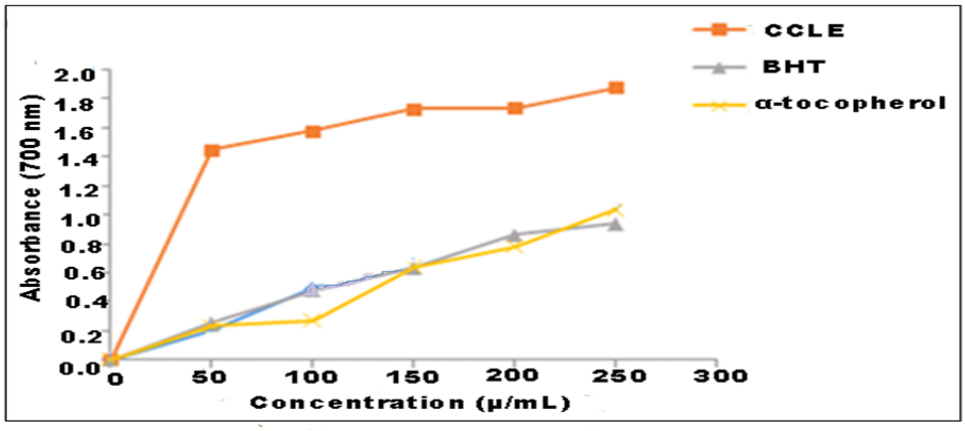

Figure 4. *The comparative reducing power assessment of BHT, a-tocopherol and CCSL ethanol extract*

3.2. Ultraviolet (UV)-visible Spectroscopic Analysis of CCS-AuNPs

UV-visible spectroscopy is one of the precious techniques for structural definition of AuNPs. It is well-known that AuNPs are anticipated to display an absorption peak in the wavelength range of 500–600 nm. In present study, after 5 min of incubation, formation of CCS-AuNPs observed by a change of the solution colour from light yellow to dark purple. Consecutive color changes within a few minutes depending on the dimension and shape of the gold nanoparticles distinctly demonstrated the production of CCS-AuNPs. Figure 5 presents typical spectra that were obtained using three different volume of CCSL extract. As shown in Figure 5, there is no peak for the CCSL extract and chloroauric acid solution in the wavelength range of 500-600 nm; however the CCS-AuNPs that produced with different volumes of CCSL concentrate formed homogeneous peaks with changing densities and amplitudes.

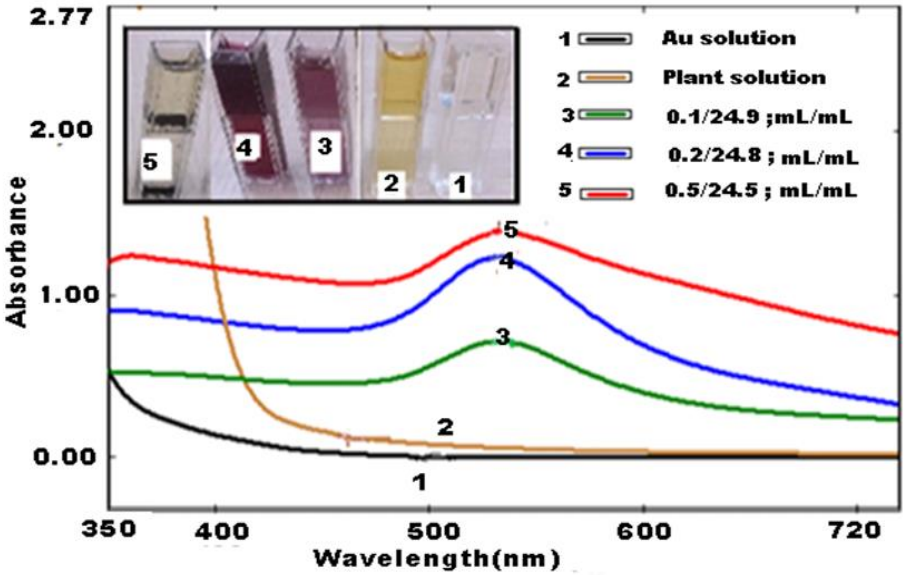

Figure 5. *Absorption spectra of(1) chloroauric acid solution, (2)CCSL extract, (3), (4)and (5)CCS-AuNPs solutions (CCSL extract /$HAuCl_4$, 0.1/24.9, 0.2/24.8 and 0.5/24.5; v/v, after one hour). The figure inset shows the corresponding color change of the solutions. Reference: Distilled water*

3.3. Effect of Different Parameters on the Production of CCS-AuNPs

Use of Au-NPs in coatings, packaging, electronics, photonics, optics, cosmetics and biomedicine is dependent on the capability to produce nanoparticles having homogeneous chemical composition, shape, size and should be chemically steady without of plant extract and $HAuCl_4$ solution. When the reaction

mixture was continuously stirred at 25°C, it was observed that the colour turned from light yellow to dark purple within 5 minutes. The absorption peaks arising from the surface optical feature of gold demonstrate exclusively at nano size, called as surface plasmon resonance (SPR). The occurrence of the SPR absorption peak (in the range of 500-600 nm) obtained for all volume ratios of plant extract/$HAuCl_4$ solution (0.1/24.9, 0.2/24.8 and 0.5/24.5, v/v) supported the production of CCS-AuNPs. Corresponding absorption spectra are presented in Figure 6.

To search formation of AuNPs over time, a series of absorption spectra were taken for three different solutions prepared at varying volume ratios (CCSL extract: chloroauric acid, i.e.,0.5:24.5, 0.2:24.8 and 0.1:24.9, v/v). Absorption spectra recorded at consecutive time intervals for 5h are shown in Figures 6a-c.

As seen in Figure 6a and b, in small CCSL extract volumes the gold surface plasmon resonance maxima were observed at 534 nm. At these extract volumes (ratios of CCLE to $HAuCl_4$; 0.2:24.8 and 0.1:24.9, v/v), the absorbance values of SPR band slowly increased with increasing of incubation time. An increased density (Figure 6a and b) can be because of increasing of the quantity of AuNPs produced as a consequence of reduction of Au^{3+} ions existing in colloidal solution. The obtained narrow homogeneous peaks demonstrate that the formation of small dimension AuNPs. Production of CCS-AuNPs slowly increased with the reaction time from 5 min to 5h. The absence of a significant shift in the SPR peak maxima during this time indicates no change in the size of the AuNPs. It is presented that the SPR peak was principally depending upon the shape and size of AuNPs [31]. Absorbance values were also measured after 48 h incubation time and it was observed that there was no increase in the peak height. This indicates that saturation is achieved in the reduction of Au^{3+} ions (Data not shown). Absorption spectra recorded for the volume ratio of 0.5:24.5 (CCSLE/$HAuCl_4$, v/v) with consecutive time intervals of 15 min were given in Figure 6c. Here, all the recorded spectra of CCS-AuNPs overlap with one other; this demonstrates that the fast production of CCS-AuNPs and the reaction (production of nanoparticles) is completed exactly within the first 15 min. Peak maxima formed at around 534 nm. The nanoparticles synthesized in a 0.2:24.8 (CCSL extract: 1mM $HAuCl_4$, v/v) volume ratio formed a homogeneous and narrow peak at 534 nm. As seen Figure 6b, because the high absorbance value indicates the production of more CCS-AuNPs and no precipitate formation was observed in the reaction medium, this ratio (0.2: 24.8, v/v) was chosen as the optimum reaction condition at 25°C and was applied for further experiments.

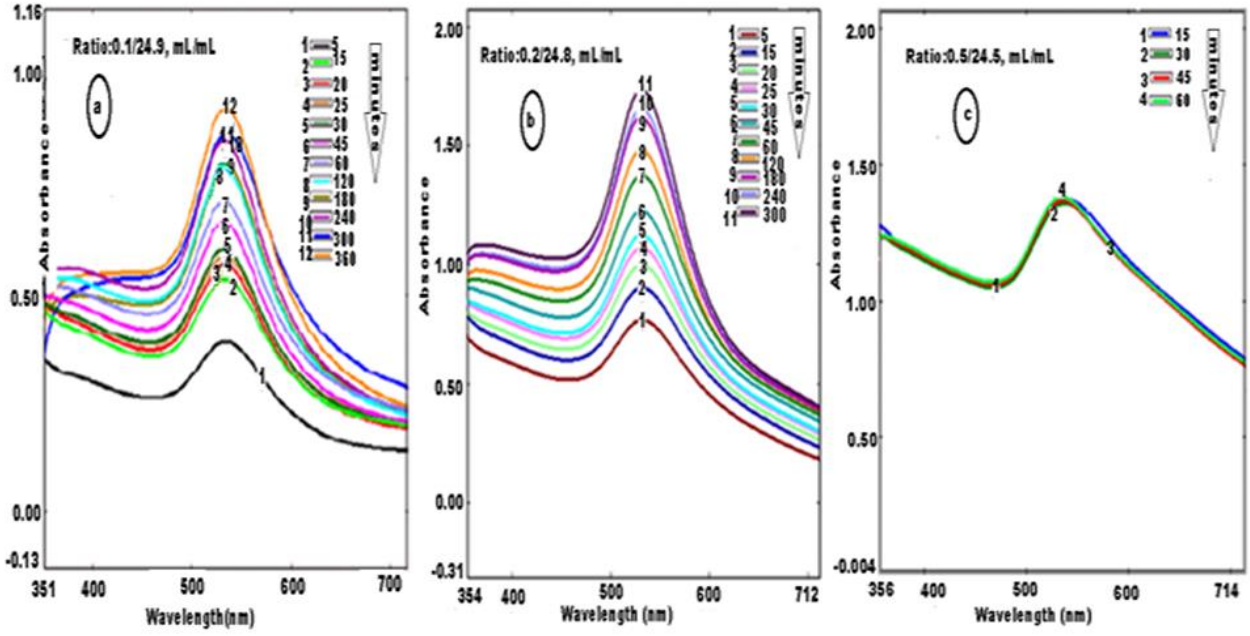

Figure 6. (a–c) *Absorption spectra of CCS-AuNPs taken at sequential time intervals and various volume ratio of CCSL extract/$HAuCl_4$ solution,* ***(a)*** *0.1/24.9,* ***(b)*** *0.2/24.8,* ***(c)*** *0.5/24.5*

As mentioned above, different parameters affect the production yields of CCS-AuNPs. Temperature is one of the most important synthesis conditions that effect the chemical features and steady AuNPs of gold

nanoparticles. The influence of temperature on the production and steady of CCS-AuNPs was investigated at different reaction times (15, 30, 45 and 60 min) and temperatures (30°C, 60°C and 90°C). Figure 7 demonstrates the impact of reaction time and temperature on the production and stability of CCS-AuNPs. At 30°C, absorption spectra of CCS-AuNPs displayed a well-characterized SPR's peak centered at around 539.2 nm, and the density regularly increased as a function of the reaction time. As seen Figure 7, at this temperature there is an initial lag time for CCS-AuNPs production and the conversion of Au^{3+} ions to Au^0 is mostly complete within 1 hour (Absorption spectra not shown). As time progresses, the absorbance value increases and the absorption spectrum becomes symmetrical with the production of homogeneous small nanoparticles. The increase in absorption intensity is due to the increase in the number of CCS-AuNPs produced due to the reduction of Au^{3+} ions present in the aqueous solution. It is seen that CCS-AuNPs peak stayed close to 539.2 nm even after 1 h of response time proposes that the nanoparticles are all around scattered in the solution and there is not excessive aggregation. As observed, the absorbance values increase with increasing temperature (at 60°C) and decrease at higher temperatures (at 90°C). Reduction was faster when the solution was heated to 60°C and to 90°C, and the purple color formed within 1 minute, but at 30°C the color change was seen after 10 minutes. It was seen that with increasing temperature from 30°C to 60°C, Au^{3+} ions were rapidly reduced to Au^0 and more CCS-AuNPs were produced. As seen in Figure 7, the reaction was completed in the first 15 minutes at 60°C. Since the maximum SPR peak density was determined during this reaction period, this temperature and time were selected as the optimum temperature and time. When the reaction time was prolonged at this temperature, an expansion in the peak and a decrease in absorbance values occurred. This indicates an aggregation of CCS-AuNP in colloidal solution. At 90°C (Figure 7), the reaction was completed before 15 min (within ~5 min). The gradual decrease in absorption peak intensities and peak broadening in course of time indicates that the colloidal solutions obtained at higher temperatures were less stable. It was observed that stable solutions could not be obtained due to aggregation in long-term reaction at high temperatures.

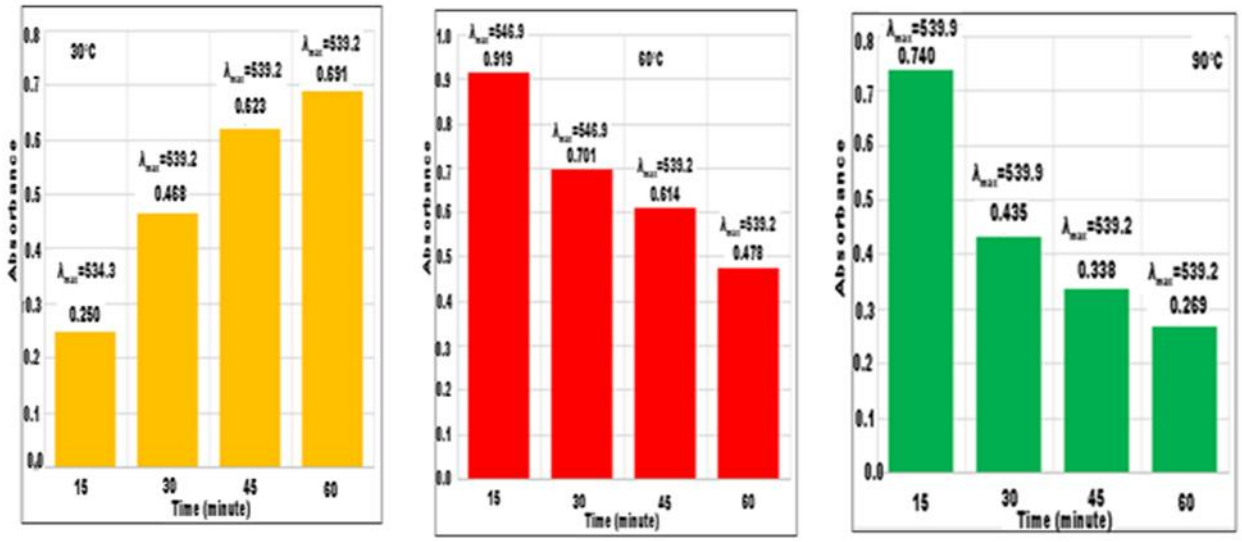

Figure 7. *Absorbance values of synthesized CCS-AuNPs at a constant incubation temperature and at different incubation time. Sample solution (CCSLE/$HAuCl_4$, 0.2/24.8, v/v, pH3)*

The subsequent factor evaluated was the pH of the reaction medium. The intensity and maximum of the SPR peaks, as well as the color of the reaction mixture, varied slightly depending on the pH. Figure 8 indicates the influence of changing pH on the production of CCS-AuNPs. There is a small change in absorption peak intensities and peak maxima, as particle sizes and amounts formed due to pH change are different. Since CCS-AuNPs produced in the pH range 3-7 are approximately the same size and homogeneous, almost no changes in peak maxima and peak shape were observed. The maximum absorption values monitored for the produced CCS-AuNPs are 537.8, 537.8, 537.8, 549.0 and 537.8 nm for synthesis pH media 3, 5, 7, 9 and 11, respectively. The peak broadening seen in the received spectrum of CCS-AuNPs synthesized at pH9 and the longer wavelength shift (from 537.8 to 549 nm, red shift) at the peak maximum indicates that the particle size increases with increasing pH (from 3 to 9). It could be said briefly that gold

nanoparticles could be produced as smaller sized particles when the pH of the solution is around 3-7. In the acidic environment, many functional groups are available for more gold complexes that bind with phytochemical compounds and allow the production of larger quantities of small diameter gold nanoparticles [32]. The decrease in peak density with changing pH values indicates that less amount of nanoparticles have been synthesized. In our study, the absorption spectra taken from time to time showed that the nanoparticles synthesized in pH7 and pH9 environments remained stable for two months, and the produced CCS-AuNPs at pH3 (particle size ~17nm) remained stable for four months. After these times, it was clearly seen that the violet color of the reaction mixture gradually began to fade and over time the CCS-AuNPs began to aggregate.

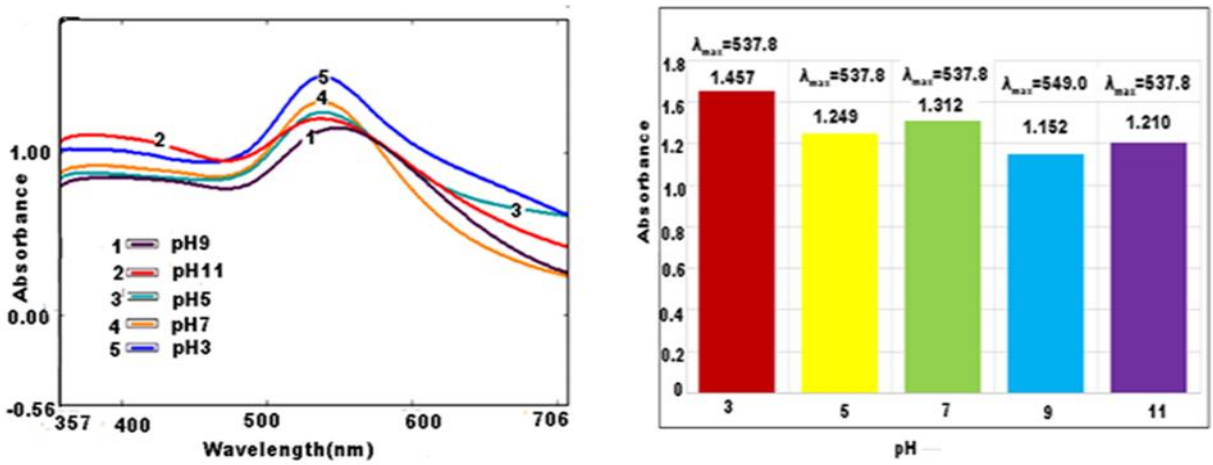

Figure 8. *Absorption spectra and absorbance values of CCS -AuNPs produced at various pH. Sample solution [CCSLE/ $HAuCl_4$, 0.2/24.8, v/v]*

3.4. Fluorescence Spectra of CCS-AuNPs

Nanometals like Au and Ag are reported to demonstrate a visible photoluminescence [33]. Fluorescent Au-NPs could be employed in sensors for the purpose of heavy metal detection, imaging, controlling the growth of pathogens etc [34]. In Au-NPs, 6sp-transmission and 5d valence band electrons have a part in fluorescence spectra [35]. It was established by Liao et al [36] and Varnavski et al [37] that in size 15 nm gold nanoparticles create fluorescent. Eichelbaum et al [38] presented that in size 10 nm gold nanoparticles show photoluminescence feature.

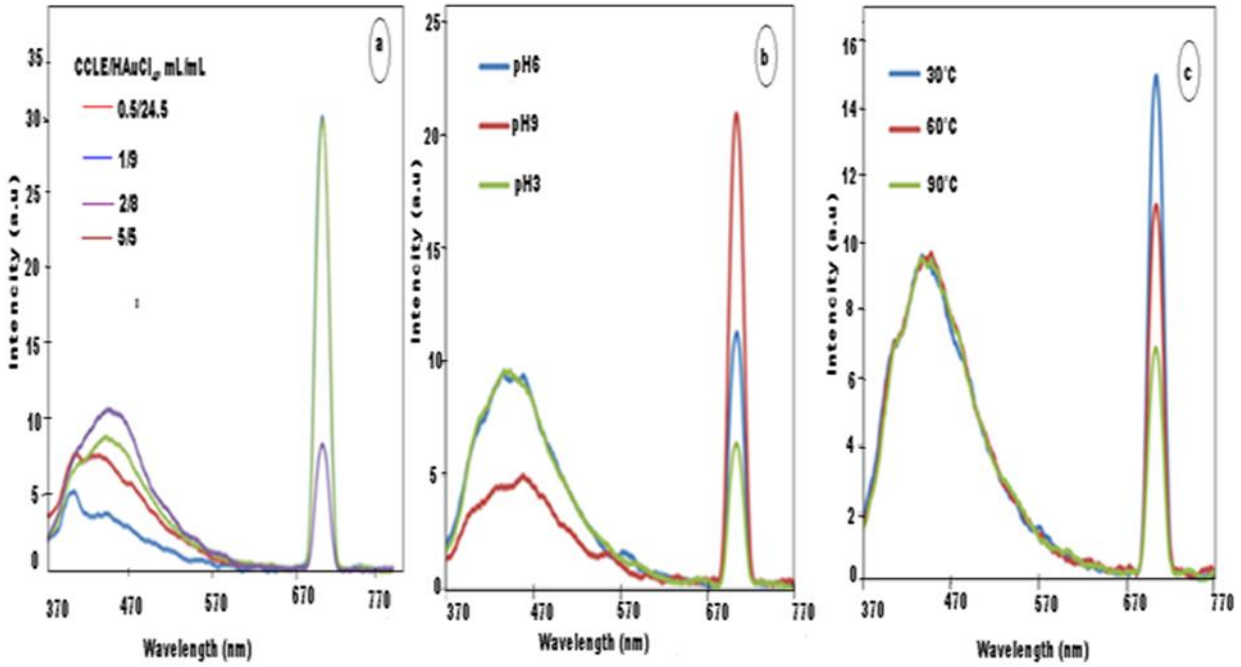

Figure 9*. Fluorescencent spectra of CCS-AuNPs as a function of* ***(a)*** *CCSL extract volume* ***(b)*** *pH* ***(c)*** *temperature (λ_{ex}=350 nm)*

The fluorescence spectra (FLS) of CCS-AuNPs synthesized as a function of CCSL extract volume are shown in Figure 9a. The FLS (λ_{exc}=350 nm) exhibits different behavior depending on the extract volume. As seen in Figure 9a, fluorescence intensity increases with increasing volume of CCSL extract. The emission spectrum shows two bands at 400 nm and 444 nm when small volume of CCSL extract was used. In using more volume of CCSL extract, the band's density at 400 nm decreases while the band density at 444 nm increases slightly. This explains that different nanostructures are formed when the low concentration of the extract is used. After adding 1 mL extract of CCSL, it is seen that the maximum of the band shifts to 455 nm. With increase of extract volume, the maximum of the SPR band was also red shifted. This study demonstrates that the band intensity and maximum of the band in the absorption spectra and fluorescence emission spectra of CCS-AuNPs are dependent on the particle size of CCS-AuNPs and extract volume of CCSL.CCS-AuNPs show another emission band at 704 nm. These emission bands (444 and 704) are because of the regional area increment through coupling to the latitudinal and longitudinal surface plasmon rebound (TSPR and LSPR, respectively) [36]. Au-NPs synthesized utilizing fresh tea leaves have also been presented [39] to act as photoluminescent through emission bands at 448 nm and 705 nm. As seen in Figure 9a, the fluorescence emission density of TSPR peak at 444 nm increases with increasing volume of CCSL extract. The density of LSPR band at 704 nm does not change with the addition of small volumes (from 0.2 mL to 2 mL) of CCSL extract, while band density decreases when volume of CCSL extract is increased (fluorescent quenching). This indicates that the quantity of CCS-AuNPs in the mixture increases as the volume of CCSL extract increases.

Fluorescence spectra of CCS-AuNPs synthesized at different reaction pH values are presented in Figure 9b. As seen, the fluorescence density of synthesized CCS-AuNPs is depended on the synthesis pH value. While the fluorescence density of TSPR band at 444 nm does not change in the acidic environment (pH3-6), it decreases (fluorescence quenches) in the basic environment (pH9). In the basic medium, the emission fluorescence peak maximum slightly shifts to longer wavelengths and the bandwidth increases. Red shift is observed in the spectrum (Figure 9b), which could be due to an increment in the particle size. The absorption peak obtained in pH9 medium supports this finding. In this environment, a more intense and broader absorption peak has been obtained and it was seen that the peak maximum shifted to longer wavelength (Figure 8).

The fluorescence spectra of CCS-AuNPs synthesized at different reaction temperatures are also shown in Figure 9c. As seen, while the fluorescent density of the TSPR band at 444 nm does not change with

increasing temperature from 30°C to 90°C, the fluorescence density of the LSPR peak at 704 nm decreases (fluorescent quenching). It was mentioned in Section 3.3 that CCS-AuNPs could be aggregated in colloidal solution at 90°C.

3.5. Fourier Transform Infrared Spectroscopic Studies of CCS-AuNPs

FTIR spectroscopic analyses were implemented for researching the possible molecules that present in CCSL extract capable for the covering, effective stabilization and reduction of the CCS-AuNPs. FTIR spectra of both CCSL extract and CCS-AuNPs were illustrated in Figure 10a and b, respectively. CCSL extract shows the absorption peaks at 3266 cm^{-1}, 1630 cm^{-1}, 1349 cm^{-1}, 1041 cm^{-1}, and 608 cm^{-1}. These detected peaks (Figure 10a) are particular for bio-molecules (such as; 3',4',7-trihydroxyflavanone, gallic acid and myricetin) which are present in CCSL extract. The intense broad -OH stretching peak at 3266 cm^{-1} confirms the existence of the –OH functional group in phenolic compounds, that may be liable for reducing of Au^{3+} ions to Au^0. The IR peak positions of CCS-AuNPs are at 3184 cm^{-1}, 1717 cm^{-1}, 1603 cm^{-1}, 1442 cm^{-1}, 1314 cm^{-1}, 1202 cm^{-1}, 1017 cm^{-1} and 755 cm^{-1}. In the case of Figure 11b, the peak at 3266 cm^{-1} shifted to low frequency (3184 cm^{-1}) and the peak density decreased. This indicates the consumption of the -OH groups during the process of reduction. The peak of -C=O tensile vibrations seen at 1630 cm^{-1} (Figure 10a) is insignificant in the spectrum of CCS-AuNPs and is divided into two peaks at 1717 cm^{-1} and 1603 cm^{-1}. This peak more occurs in phenolic molecules and demonstrating the attendance of these bio-molecules in the production of CCS-AuNPs. The peaks seen due to -C=O tensile vibrations at 1717 cm^{-1} and -C=C tensile vibrations at 1603 cm^{-1} demonstrate the probability that CCS-AuNPs binding to antioxidant compounds through the -OH and -C=O groups. Gold occurs in aqueous solutions as $[AuCl_4]^-$ ions and is an effective oxidant agent, and therefore the solution containing $[AuCl_4]^-$ ions could be used to reduce Au^{3+} ions to Au^0. After 1600 cm^{-1} to 500 cm^{-1}, positions of peaks are nearly similar with a slight shift in the band positions as those before reduction, with varying intensity. Similar research findings have been presented for production of gold and silver nanoparticles [10, 40].

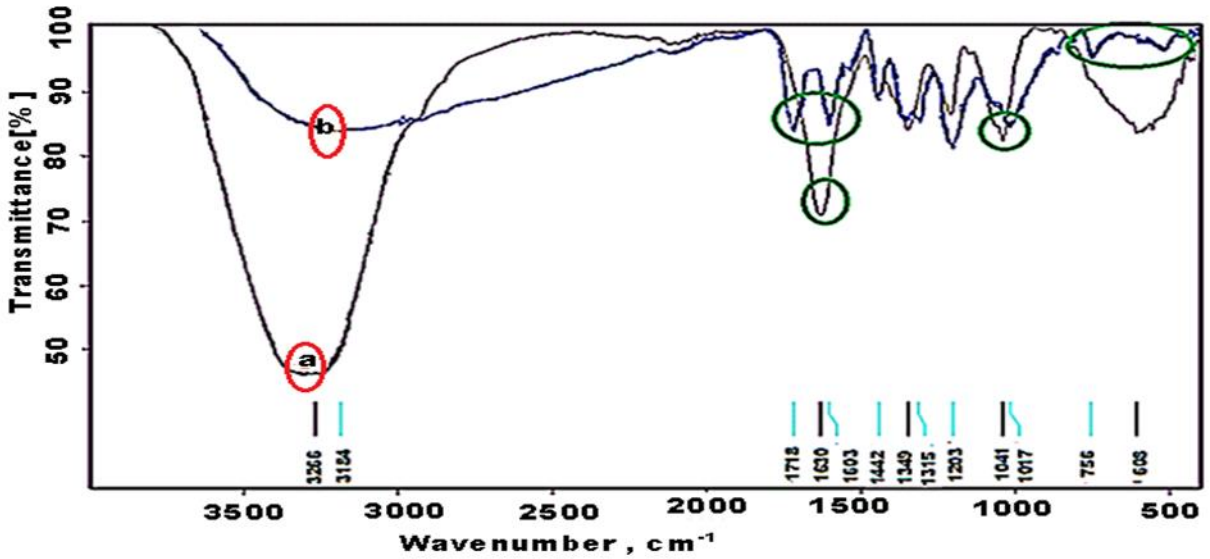

Figure 10. *FTIR spectra of* ***(a)*** *CCS leaf concentrate* ***(b)*** *CCS-AuNPs*

3.6. TEM Observations

TEM representation of produced CCS-AuNPs was shown in Figure 11a. Produced gold nanoparticles are in a spherical structure and well dispersed. This may be because of the some bio-organic molecules in the CCSL extract behave like a ligand. These molecules effectively stabilize the synthesized CCS-AuNPs, thereby controlling nanoparticle growth and aggregation. Furthermore, these molecules in CCSL extract are responsible for reducing Au^{3+} ions to Au^0. By disregarding big sized (>100 nm) particles, with the help of TEM images, mean particle dimension was measured as ~17 nm by counting over than 500 CCS-AuNPs. Smallest CCS-AuNP dimension was approximately 3.5 nm. Figure 11b shows the histogram of statistical dimension distribution of CCS-AuNPs synthesized under optimal conditions and visual of synthesized

CCS-AuNPs (Figure 11c). CCS-AuNPs prepared under these conditions remained stable for a period of four months.

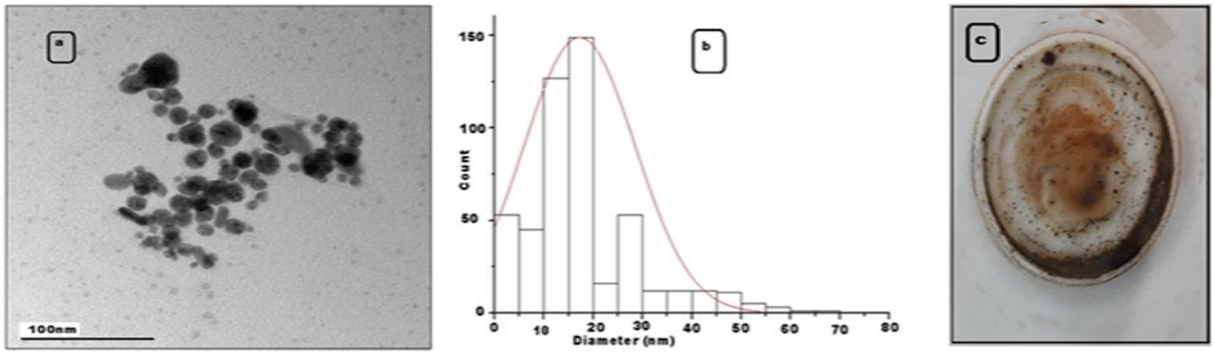

Figure 11. ***(a)*** *HR-TEM images (100µm magnification)* ***(b)*** *Histogram of dimension distribution of CCS-AuNPs* ***(c)*** *and visual of produced CCS-AuNPs*

3.7. Investigation of antibacterial efficiency of CCS-AuNPs

Synthesized CCS-AuNPs showed lower antibacterial effect than plant extract. Inhibition zone diameters of the plant extract were measured 14±1.6 mm for gram positive (*Staphylococcus aureus*) and 14±1.3 mm for gram negative (*Escherichia coli*) bacteria. CCS-AuNPs showed low antibacterial activity against both bacteria. As seen in Table 2, inhibition zone diameters of synthesized gold nanoparticles vary between 3.8 ±0.9 and 7.5±1.1 mm for *E.coli* and between 5.1±1.4 and 9.7±1.8 mm for *S. aureus.*

Table 2. *Inhibition zone (mm) obtained by the agar well diffusion procedure*

	Inhibition zone diameters (mm)	
Samples	***S. aureus***	***E.coli***
CCSL aqueous extract	14±1.6	14±1.3
CCS-AuNPs samples		
pH 3	-	-
pH 7	5.1±1.4	3.8±0.9
pH 9	9.7±1.8	7.5±1.1

Values are mean ± SE of the zone of inhibition in mm. P <0.01 as compared to the control.

The present study opens another a new route to researchers for the green production of AuNPs. In the current study, the reaction rate was high and the time required for>95% reduction of Au^{3+} ions using CCS leaf extract was approximately 10-15min. Synthesis of CCS-AuNPs that use green sources such as *Cotinus coggygria* can be an alternate to chemical production because of bio-synthesis does not contain contaminants and is friendly to the environment.

CONFLICT OF INTEREST

No conflict of interest was declared by the authors.

REFERENCES

[1] Sahoo, S.K., Parveen, S., Panda, J.J., "The Present and Future of Nanotechnology in Human Health Care", Nanomedicine, 3(1): 20-31, (2007).

[2] Kulkarni, N., Muddapur**,** U., "Biosynthesis of Metal Nanoparticles: A Review", Journal of Nanotechnology, 510246: 1–8, (2014).

[3] Mohanpuria, P., Rana, N.K., Yadav, S.K., "Biosynthesis of Nanoparticles: Technological Concepts and Future Applications", Journal of Nanoparticle Research, 10(3): 507-517, (2008).

[4] Rai, M., Yadav, A., Gade, A., "Current Trends in Phytosynthesis of Metal Nanoparticles", Critical Reviews in Biotechnology, 29(1): 78-78, (2009).

[5] Wang, Y., He, X., Wang, K., Zhang, X., Tan, W., "*Barbated Skullcup* Herb Extract-Mediated Biosynthesis of Gold Nanoparticles and Its Primary Application in Electrochemistry", Colloids and Surfaces B: Biointerfaces, 73(1): 75-79, (2009).

[6] Ponarulselvam, S., Panneerselvam, C., Murugan, K., Aarthi, N., Kalimuthu, K., Thangamani, S., "Synthesis of Silver Nanoparticles Using Leaves of *Catharanthus Roseus Linn. G. Don* and Their Antiplasmodial Activities", Asian Pacific Journal of Tropical Biomedicine, 2(7): 574-580, (2012).

[7] Liang, T., Yue, W., Li, Q., "Comparison of The Phenolic Content and Antioxidant Activities of *Apocynum Venetum L.*(Luo-Bu-Ma) and Two of Its Alternative Species", International Journal of Molecular Sciences, 11(11): 4452-4464, (2010).

[8] Satyavani, K., Gurudeeban, S., Ramanathan, T., Balasubramanian, T., "Biomedical Potential of Silver Nanoparticles Synthesized From Calli Cells of *Citrullus Colocynthis (L.)* Schrad", Journal of Nanobiotechnology, 9(1): 43, (2011).

[9] Parida, U.K., Bindhani, B.K., Nayak, P., "Green Synthesis and Characterization of Gold Nanoparticles Using *Onion (Allium Cepa)* Extract", World Journal of Nano Science and Engineering, 1(04): 93, (2011).

[10] Shabestrian H., Homayouni-Tabrizi, M., Soltani, M., Namvar, F., Azizi, S., Mohamad, R., Shabestarian, H., "Green Synthesis of Gold Nanoparticles Using Sumac Aqueous Extract and Their Antioxidant Activity", Materials Research, 20(1): 264-270, (2017).

[11] Das, R.K., Gogoi, N., Babu, P.J., Sharma, P., Mahanta, C., Bora, U., "The Synthesis of Gold Nanoparticles Using *Amaranthus Spinosus* Leaf Extract and Study of Their Optical Properties", Advances in Materials Physics and Chemistry, 2: 275–281, (2012).

[12] Islam, N.U., Amin, R., Shahid, M., Amin, M., Zaib, S., Iqbal, J., "A Multi-Target Therapeutic Potential of *Prunus Domestica* Gum Stabilized Nanoparticles Exhibited Prospective Anticancer, Antibacterial, Urease-İnhibition, Anti-İnflammatory and Analgesic Properties", BMC Complementary and Alternative Medicine, 17(1): 276-293, (2017).

[13] Singh, A.K., Srivastava, O.N., "One-Step Green Synthesis of Gold Nanoparticles Using *Black Cardamom* and Effect of pH on Its Synthesis", Nanoscale Research Letters, 10(1): 353, (2015).

[14] Parida, U., Biswal, K., Bindhani, B., Nayak, P., "Green Synthesis and Characterization of Gold Nanoparticles Using *Elettaria Cardamomum L.* Extract", World Applied Sciences Journal (WASJ), 28: 962-967, (2013).

[15] Abdel-Raouf, N., Al-Enazi, N.M., Ibraheem, I.B., "Green Biosynthesis of Gold Nanoparticles Using *Galaxaura Elongata* and Characterization of Their Antibacterial Activity", Arabian Journal of Chemistry, 10: 3029-3039, (2017).

[16] Song, J. Y., Jang, H. K., Kim, B. S., "Biological Synthesis of Gold Nanoparticles Using *Magnolia Kobus* and *Diopyros Kaki* Leaf Extracts", Process Biochemistry, 44(10): 1133-1138, (2009).

[17] Yang, N., WeiHong, L., Hao, L., "Biosynthesis of Au Nanoparticles Using Agricultural Waste *Mango* Peel Extract and Its in Vitro Cytotoxic Effect on Two Normal Cells", Materials Letters, 134: 67-70, (2014).

[18] Khalil, M.M., Ismail, E.H., El-Magdoub, F., "Biosynthesis of Au Nanoparticles Using *Olive* Leaf Extract: 1st Nano Updates", Arabian Journal of Chemistry, 5(4): 431-437, (2012).

[19] Islam, N.U., Jalil, K., Shahid, M., Muhammad, N., Rauf, A., "*Pistacia Integerrima* Gall Extract Mediated Green Synthesis of Gold Nanoparticles and Their Biological Activities", Arabian Journal of Chemistry, 12(8): 2310-2319, (2019).

[20] Islam, N.U., Jalil, K., Shahid, M., Rauf, A., Muhammad, N., Khan, A., Khan, M. A., "Green Synthesis and Biological Activities of Gold Nanoparticles Functionalized with *Salix Alba*", Arabian Journal of Chemistry, 3(8): 1-42, (2015).

[21] Tahir, K., Nazir, S., Li, B., Khan, A.U., Khan, Z. U. H., Gong, P.Y., Ahmad, A., "*Nerium Oleander* Leaves Extract Mediated Synthesis of Gold Nanoparticles and Its Antioxidant Activity", Materials Letters, 156: 198-201, (2015).

[22] Novaković, M.M., Vučković, I.M., Janaćković, P.T., Soković, M., Filipovic, A., Tešević, V., Milosavljević, S.M., "Chemical Composition, Antibacterial and Antifungal Activity of The Essential Oils of *Cotinus Coggygria* From Serbia", Journal of the Serbian Chemical Society, 72(11): 1045-1051,

[23] Matić, S., Stanić, S., Bogojević, D., Vidaković, M., Grdović, N., Arambašić, J., Mladenović, M., "Extract of The Plant *Cotinus Coggygria Scop*. Attenuates Pyrogallol-İnduced Hepatic Oxidative Stress İn Wistar Rats", Canadian Journal of Physiology and Pharmacology, 89(7): 401-411, (2011).

[24] Demirci, B., Demirci, F., Başer, K. H. C., "Composition of The Essential Oil of *Cotinus Coggygria Scop*. From Turkey", Flavour and Fragrance Journal, 18(1): 43-44, (2003).

[25] Marčetić, M., Božić, D., Milenković, M., Malešević, N., Radulović, S., Kovačević, N., "Antimicrobial, Antioxidant and Anti-İnflammatory Activity of Young Shoots of The Smoke Tree, *Cotinus Coggygria Scop*", Phytotherapy Research, 27(11): 1658-1663, (2013).

[26] Šavikin, K., Zdunić, G., Janković, T., Stanojković, T., Juranić, Z., Menković, N., "In Vitro Cytotoxic and Antioxidative Activity of *Cornus Mas* and *Cotinus Coggygria*", Natural Product Research, 23(18): 1731-1739, (2009).

[27] Akkol, E.K., Göger, F., Koşar, M., Başer, K.H.C.,"Phenolic Composition and Biological Activities of *Salvia Halophila* and *Salvia Virgata* from Turkey", Food Chemistry, 108(3): 942-949, (2008).

[28] Kano, M., Takayanagi, T., Harada, K., Makino, K., Ishikawa, F., "Antioxidative Activity of Anthocyanins from *Purple Sweet Potato*, Ipomoera Batatas Cultivar Ayamurasaki", Bioscience, Biotechnology and Biochemistry, 69(5): 979-988, (2005).

[29] Dehpour, A.A., Ebrahimzadeh, M.A., Fazel, N.S., Mohammad, N.S., "Antioxidant Activity of The Methanol Extract of *Ferula Assafoetida* and Its Essential Oil Composition", Grasas y aceites, 60(4): 405-412, (2009).

[30] Perez, C., Pauli, M., Bazerque, P., "An antibiotic assay by the agar well diffusion method", Acta Biologiae et Medicinae Experimentalis, 15(1): 113-115, (1990).

[31] Mock, J.J., Barbic, M., Smith, D.R., Schultz, D.A., Schultz, S., "Shape Effects in Plasmon Resonance of Individual Colloidal Silver Nanoparticles", The Journal of Chemical Physics, 116(15): 6755-6759, (2002).

[32] Armendariz, V., Herrera, I., Jose-yacaman, M., Troiani, H., Santiago, P., Gardea-Torresdey, J.L., "Size Controlled Gold Nanoparticle Formation by *Avena Sativa* Biomass: Use of Plants in Nanobiotechnology", Journal of Nanoparticle Research, 6(4): 377-382, (2004).

[33] Philip, D., "Biosynthesis of Au, Ag and Au–Ag Nanoparticles Using Edible *Mushroom* Extract", Spectrochimica Acta Part A: Molecular and Biomolecular Spectroscopy, 73(2): 374-381, (2009).

[34] Paul, B., Tiwari, A., "A Brief Review on The Application of Gold Nanoparticles as Sensors in Multi Dimensional Aspects", IOSR Journal of Environmental Science, Toxicology and Food Technology, 1: 1-7, (2015).

[35] Link, S., El-Sayed, M.A., "Shape and Size Dependence of Radiative, Non-Radiative and Photothermal Properties of Gold Nanocrystals", International Reviews in Physical Chemistry, 19(3): 409-453, (2000).

[36] Liao, H., Wen, W., Wong, G.K., "Photoluminescence from Au Nanoparticles Embedded in Au: Oxide Composite Films", The Journal of the Optical Society of America B, 23(12): 2518-2521, (2006).

[37] Varnavski, O., Ispasoiu, R.G., Balogh, L., Tomalia, D., Goodson, T., "Ultrafast Time-Resolved Photoluminescence from Novel Metal–Dendrimer Nanocomposites", The Journal of Chemical Physics, 114(5): 1962-1965, (2001).

[38] Eichelbaum, M., Schmidt, B.E., Ibrahim, H., Rademann, K., "Three-Photon-Induced Luminescence of Gold Nanoparticles Embedded In and Located on The Surface of Glassy Nanolayers", Nanotechnology, 18(35): 355702, (2007).

[39] Boruah, S.K., Boruah, P.K., Sarma, P., Medhi, C., Medhi, O.K., "Green Synthesis of Gold Nanoparticles Using *Camellia Sinensis* and Kinetics of The Reaction", Advanced Materials Letters, 3(6): 481-486, (2012).

[40] Ghorbani, P., Soltani, M., Homayouni-Tabrizi, M., Namvar, F., Azizi, S., Mohammad, R., Moghaddam, A.B., "*Sumac* Silver Novel Biodegradable Nano Composite for Bio-Medical Application: Antibacterial Activity", Molecules, 20(7): 12946-12958, (2015).